

# Longitudinal monitoring of sewershed resistomes in socioeconomically diverse urban neighbourhoods

**Michael Parkins**

mdparkin@ucalgary.ca

University of Calgary <https://orcid.org/0000-0003-3749-7930>

**Jangwoo Lee**

University of Calgary

**Kevin Xiang**

University of Calgary

**Emily Au**

University of Calgary

**Shahrzad Sarabi**

University of Calgary

**Nicole Acosta**

University of Calgary

**Srijak Bhatnagar**

Athabasca University <https://orcid.org/0000-0003-0240-2655>

**Jennifer Van Doorn**

University of Calgary

**Stefania Bertazzon**

University of Calgary <https://orcid.org/0000-0002-1292-5348>

**John Conly**

University of Calgary

**Elissa Rennert-May**

University of Calgary

**Johann Pitout**

University of Calgary

**Bonita Lee**

Alberta Provincial Laboratory for Public Health

**Xiaoli Pang**

University of Calgary

**Christine O'Grady**

University of Calgary

**Kevin Frankowski**

University of Calgary


**Casey Hubert**

## Article

### Keywords:

**Posted Date:** May 7th, 2024

**DOI:** <https://doi.org/10.21203/rs.3.rs-4202677/v1>

**License:**  This work is licensed under a Creative Commons Attribution 4.0 International License. [Read Full License](#)

**Additional Declarations:** There is **NO** Competing Interest.

---

# Abstract

Understanding factors associated with antimicrobial resistance (AMR) distribution across populations is a necessary step in planning optimal mitigation measures. While associations between AMR and socioeconomic-status (SES), including factors like income, employment, education, have been increasingly recognized in low- and middle-income settings, this interplay is less clear in high-income countries. We explored the relationship between SES and AMR in Calgary, Canada using spatially-resolved wastewater-based surveillance of resistomes detected by metagenomics across socio-economically diverse urban neighbourhoods. Conducting this comparison during the height of COVID-related international travel restrictions (Dec.2020-Oct.2021) allowed the hypotheses linking SES and AMR to be assessed with limited confounding. Wastewater metagenomes from eight diverse neighbourhoods exhibited highly similar resistomes, with no quantitative differences ( $p > 0.05$ ), low Bray-Curtis dissimilarity, and no significant correlations with SES. By comparison, dissimilarity was observed between globally-sourced resistomes from 244 cities ( $p < 0.05$ ), underscoring the homogeneity of resistomes in Calgary's sub-populations. The analysis of globally-sourced resistomes alongside Calgary resistome further revealed lower AMR burden in Calgary relative to other cities around the world was particularly pronounced for some of the most clinically-relevant AMR genes (e.g., beta-lactamases, macrolide-lincosamide-streptogramin). This work showcases the effectiveness of inclusive and comprehensive wastewater-based surveillance for exploring the interplay between SES and AMR.

## 1. Introduction

While antimicrobial resistance (AMR) is a global threat, its prevalence and impact exhibits significant regional variation<sup>1,2</sup>. Multiple global surveys for AMR among clinical isolates such as *Escherichia coli*, *Klebsiella pneumoniae*, and *Pseudomonas aeruginosa* reveal higher rates of AMR (i.e., as a proportion of isolates) in low- and middle-income countries (LMICs)<sup>3,4</sup>. Furthermore, recent studies investigating wastewater from large municipalities around the world to understand the resistome (i.e., all antimicrobial resistance genes (ARGs) identified in large metagenomic libraries), highlighting uneven distributions of AMR between countries aligned with geographic and social factors<sup>5-7</sup>. Several of these studies have correlated different socio-economic status (SES) variables (e.g., income, education, employment) with ARGs, highlighting the association between social determinants of health and AMR. Despite observing this pattern in low- and middle-income settings, within high income countries a similar consensus does not exist<sup>8-10</sup>. In order to identify and quantify the magnitude of AMR in any location, and assess risks between locations, programs that provide comprehensive monitoring of AMR across diverse populations are needed.

One of the hurdles in assessing potential effects of SES on AMR at the population level is obtaining data from as many individuals as possible to estimate generalized trends. The most widely used approaches for AMR surveillance involve isolating antibiotic resistant organisms from individual human and animal populations in clinical settings. Current surveillance methods generally include only individuals with active infections as opposed to those merely colonized by organisms with ARGs, and therefore underestimate the true burden of AMR. Furthermore, this approach is costly, time consuming and suffers from selection bias towards individuals receiving complex medical care or towards immunocompromised individuals and similarly excludes individuals unable to access healthcare<sup>11</sup>. Accordingly, marginalized populations may not be well represented in active

enrollment studies, limiting the generalizability of these data <sup>12</sup>. Accordingly, neither the breadth of AMR nor its contributing factors are well understood.

Many of the limitations of population sampling to understand AMR can be overcome by wastewater-based surveillance (WBS), which offers an objective, comprehensive, inclusive and unbiased way to cost-effectively monitor analytes such as ARGs <sup>13</sup>. In this study, we monitored trends of ARGs in wastewater over 11-months of longitudinal sampling of eight separate Calgary neighbourhoods (ranging from 10,000 to 80,000 individuals) cumulatively representing approximately 19% of Calgary's 1.3 million population. Neighbourhoods were selected to represent SES differences in this high-income setting <sup>14</sup>. Local Calgary resistomes were also compared with published datasets from 244 different cities worldwide with marked SES differences. Accordingly, the primary goal of this work was to quantify ARG dissimilarity between neighbourhoods and as a function of SES. The secondary goal was to provide context to the Calgary resistome relative to cities around the globe. In this way, WBS offers valuable insights into potential associations between community resistome structure and SES, as well as key ARGs over- or under-represented in different settings.

## 2. Results

### 2.1. Variable SES across eight Calgary neighbourhoods

Eight distinct neighbourhoods monitored in this study are spread across Calgary's urban area and differ with respect to SES (Table 1). In particular, median individual annual income ranged from \$26,125 to \$61,000 CAD, proportions of the population with a post-secondary degree ranged from 46 to 79%, and unemployment rates ranged from 9 to 16% (see Eq. 1–3 for calculation methods). The proportion of residents who had immigrated to Canada from another country ranged from 18 to 66% (see Eq. 4) (Fig. 1b). Among the included parameters, income and education were positively associated with each other ( $p_{\text{adj}} = 0.02$ ). Pairs that were not statistically significant but reflected expected trends ( $p_{\text{adj}}$  ranging 0.11–0.14) included positive associations ( $r > 0$ ) between education and income, and between unemployment and immigration; negative associations ( $r < 0$ ) were noted between immigration and income, immigration and education, and unemployment and education (Fig. 1c).

Table 1

Neighbourhoods monitored for wastewater-based surveillance of resistomes in Calgary, Alberta, Canada (population associated, number of samples, and collection dates).

Neighbourhood	Population	Number of Samples	Start-End of Collection
NE1	44,839	10	December 02, 2020 - August 10, 2021
NE2	18,909	9	December 02, 2020 - August 10, 2021
NE3	18,340	9	December 02, 2020 - August 10, 2021
NW1	46,008	5	June 01, 2021 - October 03, 2021
SW1	12,750	5	April 15, 2021 - August 10, 2021
SW2	13,400	4	May 13, 2021 - August 10, 2021
FP1	72,886	4	March 09, 2021 - June 03, 2021
FP2	15,385	6	Match 09, 2021 - August 17, 2021

## 2.2. Longitudinal observation of ARGs in wastewater during COVID-19-related travel restrictions

Wastewater monitoring spanned 11 months, from December 02, 2020 to October 05, 2021. During this period pandemic-related travel restrictions were in effect (Fig. S2), as reflected by an 81% reduction in international flights, and a 58% reduction in domestic flights relative to pre-pandemic levels<sup>15</sup>. We collected 52 separate wastewater samples spanning the eight monitored neighbourhoods (i.e., 4 to 10 samples per neighbourhood), from which 825 different ARGs were identified. These genes were classified into 29 different ARG types, with the most abundant type being beta-lactamase genes (327) followed by multidrug resistance genes (146) and macrolide-lincosamide-streptogramin (MLS) resistance genes (72). Clinically important ARGs that were detected included *blaOXA*, *blaTEM*, *blaCTX-M*, *blaSHV*, *blaCARB*, *qnrS* and *ermB* (Dataset S1); these ARGs are frequently identified in pathogens cultured from patient-derived samples<sup>16–19</sup>.

Quantitative comparisons of the 29 ARG types between neighbourhoods demonstrated that wastewater resistomes were relatively homogeneous and did not differ between Calgary sub-populations. Kruskal-Wallis testing followed by Wilcoxon testing indicated no significant differences ( $p > 0.11$ ) over the course of the 11-month monitoring period (Fig. 2a-b; Fig. S3-S4) for all neighbourhoods. To assess clinically significant ARGs at a more granular level, cross-neighbourhood comparisons were also performed for ARG subtypes (i.e., individual variant genotypes, e.g., *blaOXA*-1, -2, etc). This analysis showed that only nine out of the 825 ARGs differed by neighbourhood ( $p < 0.05$ ) (Fig. 2c-d), i.e., the vast majority showed no significant difference between neighbourhoods. ARG subtypes exhibiting some regional differences included one bacitracin (*bcrA*), one beta-lactam (*blaOXA*-11), one MLS (*InuD*), one multidrug (*mdtB*), one peptide (*arnA*), one phenicol (*catQ*), one pleuromutilin (*taeA*), and two tetracycline (*tet32* and *tetM*). Relative abundances of those nine ARG subtypes did not differ among neighbourhoods with different SES; rather in some situations neighbourhoods with similar SES profiles exhibited differences with respect to the relative abundance of these ARGs (e.g., NE2 vs NE3 for *arnA*, *bcrA*, and *catQ*) (Table S1). Furthermore, none of these ARGs were *a priori* hypothesized to associate with SES or to exhibit geographical variation, and their rate of association was not substantially different from what would be expected through random chance. Similarly, no significant differences in ARGs of clinical importance,

such as genes for beta-lactamases (*bla*OXA, *bla*CTX-M, *bla*SHV, *bla*TEM, *bla*CARB families), MLS (*erm*B), and fluoroquinolone resistance (*qnr*S) were observed amongst neighbourhoods as shown in Fig. 2e-f. Gene abundances for *bla*TEM and *qnr*S determined independently by complementary qPCR testing correlated significantly with metagenomic data (Fig. S5-S6), confirming these findings.

Pairwise Spearman correlation was performed to assess for potential associations between SES and ARGs, with median ARG abundance for each longitudinal data series used to represent each neighbourhood. SES did not significantly correlate with any of the selected ARGs of clinical importance (Fig. 3a), or with major ARG types (Fig. 3b).

## 2.3. ARG diversity across different Calgary neighbourhoods

Alpha-diversity analysis of ARG subtypes (Shannon index) did not significantly differ by neighbourhood based on Kruskal-Wallis testing followed by Wilcoxon testing (Fig. 4a). Beta-diversity analysis of ARG subtypes visualised using non-metric multidimensional scaling (NMDS) revealed no clustering by neighbourhood (Fig. 4b). Pairwise neighbourhood comparisons revealed that there were no statistically significant differences between any of the combination pairs (pairwise ANOSIM; Table S2), indicating that intra-neighbourhood variation was greater than inter-neighbourhood variation. A similar conclusion was derived from pairwise-PERMANOVA; Table S2), which showed centroids for the neighbourhoods did not significantly differ from each other. The same beta-diversity analysis was performed exclusively for the beta-lactam antibiotic resistance genes (Fig. 4c), and for selected beta-lactamase ARGs (*bla*SHV, *bla*CARB, *bla*OXA, *bla*TEM and *bla*CTX) (Fig. 4d). In addition, pairwise-ANOSIM and PERMANOVA showed no significant differences among neighbourhoods (Table S3 & S4). Overall, alpha and beta diversity comparisons of neighbourhood ARGs were consistent with the observations of relatively homogeneous resistomes throughout Calgary during the monitoring period.

## 2.4. ARG dissimilarity at different geographical scales: Intra-city versus inter-city variations

The magnitude of dissimilarities between wastewater resistomes is context dependent. To explore how regional sub-populations within a single city/health district sharing a common antimicrobial stewardship program compared to differences between diverse cities around the world, intra-city (within Calgary) and inter-city variations in ARG profiles were compared. Composite libraries for the Calgary neighbourhoods were amalgamated (see Methods 4.7) enabling ARGs from eight Calgary neighbourhoods to be analysed alongside 656 published sewage metagenomes from other cities around the world. This dataset together encompasses 1,418 ARGs spanning 30 different ARG types. This global analysis revealed that resistomes clustered according to Human Development Index (HDI) scores, an index that represents various SES parameters, including income and education<sup>20</sup> (Fig. 5b-5c). This clustering did not extend to resistomes from cities with similar unemployment rates (Fig. S7). Subsequent analysis using HDI as a primary SES parameter highlighted dissimilarity among Calgary resistomes in 2021 that is significantly lower ( $p < 0.01$ , using Eq. 6 in the section 4.9) than dissimilarity between global cities for any comparison category (Fig. 5), which was generally higher when comparing cities from very different categories, e.g., high- versus low-HDI scores (Fig. 5).

## 2.5. Characterization of the Calgary resistome relative to other global sewage resistomes

Significant ARG dissimilarity among cities with different HDI scores (see Fig. 6) enables examination of distinct ARGs associated with specific sites of interest, e.g., within Calgary. Ordination followed by biplot analysis using 656 data points including Calgary data from 2021 (this study) and a previously published study from 2017–2018<sup>7</sup>, revealed that among the 100 most-correlated ARGs, only 5 genes were positively associated with Calgary wastewater (Group-1 in Fig. 6c; see Fig. S8). These ARGs are enriched while the remaining 95 (Group-2 in Fig. 6c) were significantly diminished in the Calgary metagenomes relative to other global metagenomes (Fig. 6d; Figs. S8-9). Negatively correlated Group-2 genes included many clinically important ARGs, including several beta-lactamases (e.g., *ampC*, *bla*TEM-1, -19, -125, *bla*OXA-9, -10, -17, -240, -251, *bla*SHV-1, -67, -95, etc) (Fig. S9). Group 2 ARGs were consistently diminished in Calgary, suggesting a greater influence of the overarching factor (i.e., HDI), when compared to many other cities, particularly associated with different classifications (i.e., low HDI).

## 3. Discussion

### 3.1. Relating disease occurrence with social determinants of health via WBS

Several studies have explored how societal metrics associate with ARG prevalence<sup>8,9,21,22</sup>. Most studies reporting significant association between SES and AMR have been performed in low- and middle-income countries (LMICs), notable for high socio-economic disparities<sup>21,22</sup>. Meanwhile, studies in high-income countries have demonstrated contradictory results<sup>8,9</sup>, necessitating further exploration. Studies doing so at a more granular geospatial, neighbourhood level-scale are much less common, with recent examples emerging in the context of COVID-19 surveillance<sup>23–25</sup>. This included a study of Calgary wastewater sampled from socio-economically diverse neighbourhoods, revealing significant associations between SES variables and SARS-CoV-2 RNA levels during the COVID-19 pandemic<sup>24</sup>.

The present study demonstrated WBS at a high spatial resolution could be used to investigate potential relationships between SES and wastewater resistomes in a city within a high-income country, Calgary. Notable benefits of this study design include universally healthcare in Canada being available to all citizens. Residents can receive care at any hospital, and from any practitioner who all operate under a single service provider without restrictions (Alberta Health Services). As greater income inequality often exists within as opposed to between cities in high-income countries, a municipality focused approach increases the SES contrast between monitored sites<sup>26</sup>. With a population of over 1.3 million people, Calgary is Canada's fourth largest and second most ethnically diverse city<sup>14</sup>. Furthermore, Calgary exhibits notable disparities in SES throughout different areas of the city, as evidenced by its rank as having Canada's second highest Gini index (i.e., measure of income inequality)<sup>27</sup>. Additionally, the study period coincided with markedly diminished international travel<sup>15</sup> resulting from federal and provincial COVID-19 related restrictions that have been effective since the beginning of pandemic on March 2020<sup>28</sup>, minimizing the confounding effects of travel and the importation of AMR genes<sup>8,29</sup> during this time. A notable limitation to neighbourhood-scale WBS relates to the critical assumption that

measured analytes are ascribed to residents living within that particular sewershed catchment. However, within a large city, people are highly mobile and while most individuals report to defecate at home in the morning, significant variation can still exist <sup>24,30</sup>.

## 3.2. Homogeneous distribution of ARGs across socio-economically diverse Calgary neighbourhoods

No significant difference in ARG profiles was observed between socio-economically diverse neighbourhoods in Calgary, suggesting that SES factors (excluding international travel) do not strongly influence the spatial distribution of AMR in a high-income settings. The lack of association between AMR and SES (see 2.3) has also been observed when evaluating aggregate clinical specimens collected from clinical family practices in Rotterdam, Netherlands and three hospital zones across northern Australia <sup>8,9</sup>; similar to Calgary, these other high-income regions also have access to well-funded public health care. In contrast, AMR studies performed in LMICs reported the opposite, observing significant associations between SES and ARGs in Chilean and Brazilian hospitals <sup>21,22</sup>.

Discrepancies in the observations between HIC and LMIC in the examples above, including the present study, might be explained by differences in the types and quality of medical care, associated antibiotic prescribing practices. The successful dissemination of antibiotic stewardship teaching to clinicians and implementation of robust antibiotic stewardship programs has been widely reported in high-income countries. Indeed, many national hospital accreditation programs now mandate these programs <sup>31,32</sup>. As a result, global antibiotic consumption has dropped significantly in recent decades, especially in HICs, including Canada <sup>33</sup>. Under the assumptions that: (1) the city has established a vigilant surveillance program for antibiotic prescription/consumption; (2) the general population receives similar access to and clinical care regardless of SES; (3) there is minimal or stable external influx of AMR determinants from the outside as evidenced by significantly low-levels of international travel for the year 2021 (> 80% lower than pre-pandemic levels) <sup>15</sup>, we speculate that the population resistome, on average, experienced similar degrees of selection pressure, thus could have high similarity irrespective of SES.

Our study shows that differences in the resistomes and dissimilarity of ARGs within Calgary was small. ARGs were relatively homogenous among neighbourhoods compared to the differences observed among cities from around the world having different HDI scores (see 2.4). This may be related to the relatively equal access to health services – an important SES factor for AMR according to Wozniak, Cunningham, Ledingham and McCulloch <sup>8</sup>. In Calgary (and all of Alberta), all healthcare services are provided through Alberta Health Services, a single publicly funded health system which maintains a single antibiotic stewardship program <sup>34</sup>. Accordingly, formulary restrictions and educational interventions designed to promote responsible prescribing are equally distributed throughout the entirety of the province, and clinicians working within. Furthermore, residents can seek out any primary care provider throughout the city, or attend any urgent care, emergency room and be hospitalized accordingly <sup>34</sup>. In cities in other countries, however, access to health services may differ by location, income, health insurance status, or other factors. In other settings, standardized efforts for antibiotic stewardship may not have the same influence over the population, and marginalized groups may be excluded <sup>35</sup>. Furthermore, despite inequality observed within Calgary being high within Canada (Gini index of 0.3) it is relatively low compared to many other cities in high-income countries with publicly funded health



systems but greater income disparity (e.g., London and Paris have Gini index values of 0.58 and 0.5, respectively) possibly limiting the ability to detect any associations between SES and AMR prevalence via wastewater<sup>36</sup>. Our global resistome analysis revealed dissimilarity to be especially high when comparing cities from two highly different groups (e.g., high-income versus low-income groups; Fig. 5) compared to the more moderate (in the global context) inequality existing between Calgary neighbourhoods. An important limitation here is that comprehensive city-level data on HDI is generally not available within a single curated database, unlike country-level data<sup>20</sup>. Accordingly, we inferred country-level HDI to describe individual cities which will may not fully reflect of the economic status of those locations<sup>27</sup>.

Another important caveat to the lack of observed geospatial heterogeneity in AMR across SES diverse Calgary neighbourhoods pertains to this study being conducted during the COVID-19 pandemic with its related travel restrictions. Travel-related importation of AMR genes has previously been associated with the occurrence of many AMR infections (i.e., *Enterobacteriales* that produce extended spectrum beta-lactamases<sup>37</sup> and metallo beta-lactamases<sup>38</sup>). Under the following assumptions that: (1) immigrants settle disproportionately across the city (i.e., evidenced by significantly different country of origin by neighbourhood; Fig. S10), (2) preferred travel destinations are often influenced based on one's country of origin (i.e., more likely to return to country of origin for purposes of visiting friends and relatives)<sup>39</sup>, (3) ARGs, especially locally over-represented genes, can be imported via travel<sup>29</sup>, the dissimilarity of ARGs among neighbourhoods could be different during a period of resumed international travel.

Lower antimicrobial prescribing during the COVID-19 pandemic may have reduced the overall selection pressure for AMR, and thus could limit dissimilarities in resistomes between neighborhoods. Overall antibiotic dispensation in community pharmacies was lower in 2020 both regionally in Calgary as well as nationally<sup>40</sup>. For example, consumption of community-dispensed antibiotics in the Canadian Prairies region in 2021 were 57%, 40%, and 27% lower than the pre-pandemic levels (2019 for macrolides, penicillins and fluoroquinolones, respectively<sup>40</sup>. Nationally, the rate of community-dispensed antibiotic prescriptions decreased by an average of 26.5%, in the beginning of COVID-pandemic (the first 8 months)<sup>41</sup> then gradually increased in 2021, returning to levels comparable to those observed before the pandemic, after the wastewater sampling period in this study. Similarly, a meta-analysis of pharmaceutical sales data from 72 countries (including Canada) during 2020–2022 found similar trends across countries<sup>42</sup>. Additional AMR studies after the lifting of COVID-19-related travel restrictions to explore confounding influences arising from SES, international travel and prescribing patterns, are warranted, and will expand on the findings presented here.

### **3.3. Distribution of clinically important ARGs in wastewater around the globe and within Calgary**

Analysis of wastewater metagenomes from cities around the world confirmed that ARGs are unevenly distributed around the globe. Indeed, many studies to date have used WBS to monitor sewage-borne ARGs and found disproportionate distribution across different geographic locations<sup>5,6</sup>, or along socio-economic gradients<sup>5</sup>. Our study employing multivariate testing uniquely identified a list of key AMR determinants that were disproportionately diminished (or in a minority of situations - increased) in Calgary, or other cities with high HDI (in 2.5). In particular, several clinically important ARGs<sup>43</sup> were identified to be distributed disproportionately along the gradient of SES (i.e., HDI).

In Calgary, key ARGs of clinical importance (e.g., beta-lactamase genes including *bla*CARB, *bla*CTX, *bla*OXA, *bla*SHV and *bla*TEM, and other genes such as *qnr* and *mcr* families) were less abundant relative to other cities, particularly cities in low-HDI countries. This may relate to lower levels of antibiotic prescribing manifesting from successive antibiotic stewardship efforts in Canada, which are comparable to those in Europe<sup>44</sup>. Consumption of antimicrobials per capita in Canada was lower than the average in 29 European Union/European Economic Area (EU/EEA) countries. In particular, lower levels (measured in defined daily dose (DDD)/1,000 residents/day) of quinolones (1.7), MLS (2.9), penicillins (5.9), and other beta-lactam antibiotics (2.6) were observed relative to the EU/EEA average, which was reported as 2.0 (quinolones), 3.2 (MLS), 9.6 (penicillins), and 3.7 (other beta-lactam antibiotics) DDD/1,000 residents/day<sup>45</sup>. Owing to Canada's investment in robust antibiotic stewardship, antibiotic consumption has gradually decreased in every region across the country – especially the major classes such as beta-lactam antibiotics and macrolides/lincosamides – since 2017<sup>44</sup>. This too has been documented in Alberta (where Calgary is the largest city) where antibiotic consumption did not differ substantially from the national average<sup>46</sup>.

## 4. Materials and Methods

### 4.1. Description of neighbourhoods monitored and wastewater sampling regime

We have been able to advance and innovate WBS at a granular scale owing to a number of local advantages: (i) Calgary is unique as compared to many cities and maintains separate stormwater and wastewater collection systems (preventing human released ARGs from being diluted by stormwater); (ii) Calgary operates using a single municipal utility provider, enabling consistency in sample collection procedures; (iii) the Urban Alliance is a longstanding partnership between the University of Calgary and the City of Calgary allowing for rapid collaboration on matters relevant to societal health<sup>47</sup>. Wastewater samples were collected from a total of eight neighbourhoods in Calgary, Canada (Fig. 1a). Locations were chosen based on accessibility to sampling sites, population size, and in order to achieve a diverse cross-section of the city's population<sup>24</sup>. Sampling was performed during the COVID-19 pandemic from December 02, 2020 to October 05, 2021 (Table 1), yielding 4–10 longitudinal ~ weekly samples for each neighbourhood. We followed previously described procedures to collect composite wastewater samples<sup>24</sup>. In brief, wastewater autosamplers (ISCO5800 or ISCO6712) were deployed at manholes selected to sample the flow of sewage from the targeted catchment. The wastewater from these sites is exclusive to the population in each respective catchment (Fig. 1). The autosamplers were programmed to collect composite samples by obtaining 100mL in every 15 mins for 24 hours. Samples were shipped to the laboratory at the end of the 24-hour period and stored at -20°C until further analysis. Details on the sampling sites, and their respective populations is detailed in Table 1.

Supplementary sampling was conducted post-hoc from samples collected at the Bonnybrook Wastewater Treatment Plant (WWTP), serving a population of ~ 900,000 (> 80% of the total population of Calgary) mainly to assess a potential study-to-study variation when comparing our results with other published metagenomes (see 4.7). Three samples were obtained, and used as controls, e.g., Calgary-2022-Jan (26 Jan 2022), in the midst of COVID pandemic; Calgary-2022-Jul (July 06 2022) and Calgary-2022-Nov (23 Nov 2022), after the lifting of COVID restriction. The post-hoc sampling was performed in a same way, as detailed above.

## 4.2. Determining the socio-economic status of monitored neighbourhoods within Calgary

To establish the SES parameters of the monitored neighbourhoods we used data extracted from the Government of Canada's 2021 Census <sup>48</sup>, using the software Beyond 20/20 Professional Browser release 7.0.5092(32) (Beyond 20/20 Inc., Ottawa, Canada). Detailed extracted variables we assessed fell into the following specific categories: income related (average household size, and median total income of household), education related (the populations with, and without postsecondary degrees or equivalent), and unemployment related factors (unemployed population, and total labour force). Immigration status is known to be another factor that could be associated with SES <sup>49</sup> – immigration related factors such as generation status for the population (first, second, third or more generation), and the place of birth for the recent immigrant population were also extracted. The aforementioned data were accessible at each defined area (DA) level, as determined by the national statistical agency. These DAs were defined at a granular (zoomed-in) scale. Consequently, aggregating multiple DAs provided an imperfect approximation of the entire sewage catchment area (Fig. 1a). Notably, several sewersheds captured modest areas of parks, recreational and industrial sites in addition to the sought large residential areas of study. As a result, we calculated the median of values for multiple DAs, which was then subjected to further analysis, as detailed below.

**(Eq. 1) Median total income of household per capita (CAD)** = Median total household income/Average household size

**(Eq. 2) Education rate** = Population with a postsecondary degree (or equivalent)/Total population with and without postsecondary degrees

**(Eq. 3) Unemployment rate** = Unemployed population/Total labour force

**(Eq. 4) Immigration rate** = Number of first-generation immigrants/Total population

Subsequently, the median values for the abovementioned parameters were calculated for each neighbourhood, then used when correlated against ARG data.

## 4.3. Understanding the confounding of air travel in to Calgary during the study

The amount of air travel was estimated using the number of passengers arriving at the Calgary international airport from 2018 to 2022 extracted from Statistics-Canada <sup>15</sup>. The yearly aggregated data were extracted from the database, for each sector, namely domestic (flights within Canada), transborder (flights between Canada and the USA), and international sectors (flights between Canada and countries other than the USA) (see Fig. S2).

## 4.4. Sample processing and DNA extraction

Samples were thawed at 4°C overnight, and after thorough mixing 80 mL aliquots were removed and centrifuged (4,200 rpm at 4°C for 20 minutes). Supernatant was removed, and the volume of the remaining pellets was recorded (~ 0.5 to 7.2mL depending on the amount of pellet) and used for further calculation (i.e.,

percentage of raw wastewater volume processed for DNA extraction). Aliquots of 250µL of the resuspended pellets (corresponding to 5 to 36 mL of raw wastewater) were subjected to total genomic DNA extraction using the PowerSoil DNA Isolation Kit (Qiagen, Germany) in a final elution volume of 50 µL. DNA (260/280 and 260/230 absorbance ratios) was measured using Nanodrop (Thermo Fisher Scientific, USA) and concentrations were determined by fluorometry using a Qubit™ dsDNA High-Sensitivity Kit (Thermo Fisher Scientific, USA). Extraction blanks were included in every batch to assess for contamination, resulting in concentrations always below the detection limit (< 0.1ng/µL). Extracted DNA samples were stored at -70°C until further analysis.

## 4.5. Shotgun-sequencing and metagenomic analysis for neighbourhood samples

Library preparation and shotgun sequencing were performed by Novogene Corporation Inc., California, USA (<https://www.novogene.com/us-en/>) on an Illumina Novaseq 6000 with paired-end 2×150bp strategy. Output targets were 10 gigabases (~ 33M paired reads) per sample, and the final outputs ranged from 10.1–17.8 gigabases (median = 13.0, IQR = 11.9–14.0 gigabases) (Dataset S2), yielding 0.85 (IQR: 0.82–0.88) estimated average coverage, calculated using Nonpareil (v3.303) <sup>50</sup> (Fig. S11). Raw reads were initially filtered by the sequencing provider under the following criteria for removal: (1) reads containing adapters, (2) reads containing N > 10%, (3) reads with low quality (Qscore < = 5). The qualities of processed reads were double-checked using FastQC (v.0.11.9) <sup>51</sup>, and further filtered using Trimmomatic (v0.39) <sup>52</sup>. Filtered reads were then further analyzed using the DeepARG-SL pipeline v2.0 <sup>53</sup>. This pipeline aligned reads against its database that draws ARG and 16S rRNA gene sequences from multiple public databases (i.e., CARD, ARDB, UniProt for ARGs; Greengenes for 16S rRNA genes) <sup>53</sup>. We then calculated relative abundance (ARGs per 16S rRNA gene) according to a customized workflow written in Python (v3.5.3) with Pandas (v0.25.3). The detailed workflow has been described elsewhere <sup>54</sup>. Specifically, ARG copies were calculated by the following equation,

$$copy = \frac{\text{ThenumberofreadsassignedtoeachARG} \times \text{Readlength}(bp)}{\text{Lengthofreference}(bp)} \quad (\text{Eq. 5})$$

The calculated copies for ARGs were further normalized by 16S rRNA gene copies (calculated in the same way, using Eq. 5) as described in other studies <sup>54–56</sup> in order to account for variations in fecal bioburden between samples/sites.

## 4.6. Quantitative assessment of specific ARGs

Selected ARG sub-types were also detected and quantified using independent qPCR assays targeting *qnrS* families <sup>57</sup> and *bla*TEM families <sup>58</sup>. Assay methodology has been described elsewhere <sup>54,57,58</sup>. Reaction volumes of 10 µl contained the following components: TaqMan® Fast Advanced Master Mix (Applied Biosystems, USA) (5µl), primers (final concentration = 650nM for *qnrS*, and 400nM for *bla*TEM), probes (final concentration: 250nM for *qnrS*, and 200nM for *bla*TEM), 1:5 pre-diluted template (2.5µl) and DNase/RNase-free distilled water. Assays were conducted under the following conditions: 50°C for 3 mins and 95°C for 20s (*qnrS*) or 2 mins (*bla*TEM); 40–45 cycles of 95°C (*qnrS*) or 94°C (*bla*TEM) for 1s followed by 60°C for 20 s (*qnrS*) or 1 min (*bla*TEM). The following gBlocks™ gene fragments were synthesized from Integrated-DNA-Technologies, USA, and used as standards: *bla*TEM-1 (GenBank accession no. V00613.1; fragment size = 164bp) <sup>58</sup>, and *qnrS4* (GenBank accession no. FJ418153.1; fragment size = 197bp) <sup>57</sup>. 16S rRNA genes were also analysed as

normalization markers for overall bacterial load following our previous study<sup>54</sup>. In short, qPCR assays were run using a universal primer/probe for V3-4 hypervariable regions of 16S rRNA gene<sup>59</sup> under the following conditions: 50°C for 2 min and 95°C for 2 min; 40 cycles at 95°C for 1 s followed by 62°C for 20 s. As a standard for 16S rRNA gene, *Pseudomonas aeruginosa* PA01 genomic DNA was used. Each sample and standard were run in triplicate, and all runs included no-template controls. All qPCRs were performed using QuantStudio 5 Real-time PCR systems (Applied Biosystems, USA).

The qPCR results were subject to further quality control steps, referring to relevant references<sup>56,60,61</sup>. These steps included: (1) determining the limit of quantification (LOQ) at the last dilution where standard deviation of Ct is < 0.5, (2) Ct for non-template controls were always > LOQ's Ct, (3) samples with Ct standard deviations > 0.5 among technical triplicates were not used (labelled as 'detected but not quantifiable'), (4) samples with average Ct among replicates < LOQ were not used (labelled as 'detected but not quantifiable') and (5) samples which did not show signals or showed only 1 out of 3 signals were not used (labelled as 'not detected'). Key quality parameters for standard curves were provided in Table S5. Relative abundance (ARGs per 16S rRNA gene) was calculated for quantifiable samples.

## 4.7. Analysis of global metagenomes

We searched for sewage metagenomes from around the world in the public databases (i.e., NCBI- Sequence Read Archive and European Nucleotide Archive), using keyword searching ('sewage'), then selected studies to include that met the following criteria: (1) the raw data were generated in recent 5 years (i.e., from 2016) from the beginning of this project in 2021; (2) the project included multiple countries, across different continents; (3) the raw data included the samples with a sequencing output of > 4 giga-bases, ensuring the estimated coverage of > 0.5, predicted using Nonpareil curves of 52 neighbourhood samples in this study (Fig. S11). As a result, a total of 656 sewage metagenomic samples from two projects, representing 244 cities within 101 countries collected between 2016–2018, were downloaded<sup>5,7</sup>. Details were provided in Dataset S2. These data included four additional raw sewage metagenomes from a wastewater treatment plant in Calgary from 2017–2018 (run accession IDs at ENA : ERR2683154, ERR4682435, ERR4682830, and ERR4678657). Samples varied significantly in sequencing output (see Dataset S2). To ensure accurate quantification of ARG reads across samples in downstream analysis, with a consistent limit of detection, the raw data were rarefied with 4 giga-bases outputs, yielding estimated average coverage of 0.60 (IQR: 0.54–0.67), using Seqtk (v1.3)<sup>62</sup> referring to other relevant studies<sup>63,64</sup>.

Data for key SES parameters for global resistomes, such as Human Development Index (HDI) that represents society's achievement in human development, broadly including dimensions of economic, education, and health<sup>20</sup>, and unemployment rate were obtained from the World Bank<sup>36</sup>, and United Nations Development Programme<sup>20</sup>. In principle, the values corresponding to the year of collection for global metagenome samples were compiled and subsequently averaged for each country, resulting in a singular represented HDI value for each country. Then, samples were categorized in our sample list (a total of 101 countries) into four levels for each parameter under the following rationale: High  $\geq$  Q3 (75%), Q3  $\geq$  upper middle  $\geq$  Q2 (median; 50%), Q2  $\geq$  lower middle  $\geq$  Q1 (25%), and Q1  $\geq$  low, as graphically detailed in Fig. S12.

To compare ARG dissimilarity at different geographical scales (i.e. intra versus inter-city variations; see 2.4), the 52 metagenomes from eight Calgary neighbourhoods were distilled into eight data points where each

neighbourhood was represented by a single data point, by using the median of the longitudinal datasets (up to 10) for each ARG subtype, followed by beta-diversity analysis alongside 656 global metagenomes. Similarly, to characterize ARGs profiles specific to Calgary, the 52 Calgary metagenomes were amalgamated into a singular data point (see 2.5). This analysis was based on the assumption that the singular data point represents the entire population, considering homogenous resistomes that neighbourhood samples exhibited over the course of monitoring. Subsequently, multivariate analysis was followed to analyse key determinants, associated uniquely with the Calgary resistome. Several uncertainties may impact this comparison; (1) technical errors, arising from variations in analysis workflows between our study and other published metagenomes; (2) a bias, which may arise when comparing the resistome of sub-population (i.e., neighbourhood samples) to that of the entire population (i.e., city samples from global metagenome libraries); (3) temporal variations, caused by the diverse years during which samples were collected (i.e., 2021 in this study vs 2017–2018 for other published data). To understand the sources of uncertainty, we performed a meta-analysis, including a total of 7 additional wastewater samples, obtained from a municipal wastewater treatment plant (serving > 80% populations within Calgary) as controls. The control samples were used only in pre-test (Fig. S1), but not in the main analysis (Fig. 5–6) to prevent potential skewing of overall patterns, particularly in ordination analysis, due to unbalanced sample numbers. Four control samples were analysed during comparable periods (May-26, July-06, November-23, and December-07 2022, respectively), aligned with those obtained from global metagenome libraries (June-13 2017, June-26 2018, November-21 2017, and December-10 2018, respectively). The other three samples were analysed during a comparable period (i.e, before the major shift of pandemic-related measure on Mar-01 2022; Jan-26, Feb-09, and Feb-16 2022), aligned with our 52 neighbourhood samples. Additional details regarding the selection of control samples, as well as the rationale behind the control assessment, can be found in the Supplementary-Method. Our analysis, described in the Supplementary-Method, proved that all three errors do not exist profoundly, or at least were overshadowed by the greater influence of the overarching factor (i.e., HDI) – we therefore proceeded further downstream analysis, comparing Calgary neighbourhood resistomes with the 656 global metagenomes.

## 4.8. Statistical analysis

To assess for differences among Calgary neighbourhoods, Kruskal-Wallis test was performed initially to assess whether there was a difference across groups, followed by Wilcoxon test to identify which pair(s) exhibited significant differences, using the R package 'stats (v4.1.2)'<sup>65</sup>. Alpha-diversity was measured using the Shannon index, and was performed in R using the package 'vegan (v2.6-4)'<sup>66</sup>. Dissimilarities between samples were calculated using Bray-Curtis distance, and visualized using non-metric multidimensional scaling (NMDS), which was performed using 'vegan (v.2.6-4)'<sup>66</sup>. Pairwise analysis of similarities (ANOSIM), and permutational multivariate analysis of variance (PERMANOVA) were performed to test for significant differences in dissimilarity between groups using 'vegan (v2.6-4)' and 'ecole (v.0.9)' in R<sup>67</sup>. Procrustes analysis was performed to test for structural correlations between two different ordinations using 'vegan (v2.6-4)'. Biplot analysis was employed to determine which ARG-subtypes correlated most to the ordination, and *r* and the corresponding *p*-value for each ARG were calculated via permutation (*n* = 9999) using 'vegan (v2.6-4)'<sup>66,68</sup>. To identify ARGs associated uniquely with Calgary, we calculated the residual sum of squares (RSS) for each regression line against a total of 5 data points representing Calgary (a single amalgamated data point for 2021 samples in this study, as delineated in 4.7, also 4 published Calgary metagenomes), chose the top 100 ARGs with lowest RSS as distinctive determinants uniquely linked to Calgary, then further visualized using heatmap.

The heatmaps were generated using 'gplots (v3.1.3)' in R<sup>69</sup>. The p-values for multiple comparison were corrected according to the Benjamini-Hochberg procedure using 'stats (v4.1.2)' in R<sup>65</sup>. Regression analysis was performed to test association between metagenomics and qPCR results using 'stats (v4.1.2)'<sup>65</sup>. All the graphics were generated using basic embedded functions in R (v4.1.2).

## 4.9. Monte-Carlo Permutation Simulation

Monte-Carlo permutation simulation was performed to compare dissimilarity among Calgary-2021 wastewater samples with dissimilarity among cities from around the world as follows: (1) a total of 28 pairs (= every possible combination for the 8 neighbourhoods,  $C_2^8$ ) of Bray-Curtis distance between global cities were randomly sampled from each comparison category (Fig. 5a), e.g., distance between a high HDI city versus an upper middle HDI city, a high HDI versus a lower middle HDI city, etc, (2) the median value for each comparison category was compared with the median dissimilarity between Calgary-2021 samples (Fig. 5b), and (3) the previous steps (1–2) were repeated by  $n = 100$ , then p-value (Eq. 6) was computed (Fig. 5c).

$$p = \frac{n[x|\bar{d}_{City,x} > \bar{d}_{Neighborhood}]}{n[x]} \quad (\text{Eq. 6})$$

Where,  $x$  indicates the number of simulations run (i.e., 1, 2, ... 100),  $\bar{d}$  indicates dissimilarity distance between two selected nodes.

The simulation was performed using a customized workflow in R modified from our previous study<sup>70</sup>, which is available on GitHub (<https://github.com/myjackson/permutation-simulation-for-intra-vs-intercity-variations>).

## 4.10. Ethics

This study received approval from the Conjoint Research Health Ethics Board of the University of Calgary (REB20–1544 and REB21-2025).

## Declarations

Data availability

Raw metagenomic sequencing reads were deposited in NCBI-SRA with BioProject ID of PRJNA1084884 (Reviewer link : <https://dataview.ncbi.nlm.nih.gov/object/PRJNA1084884?reviewer=ah11n6j67nce400soev7hqlrkc>). Key processed datasets were suggested in 'Supplementary Dataset' of this manuscript. The other datasets (not-shown) could be provided upon reasonable requests to the authors.

Acknowledgements

We are grateful to Rhonda G. Clark, Maria A. Bautista, Barbara J. Waddell, and Kristine Du for technical assistance. We also thank to all the other members of Pan-Alberta Wastewater-based Surveillance Network for discussion, and/or technical assistance. We are thankful for the efforts of the City of Calgary and in particular members of Water Services Department for their excellent support on provision of samples, and infrastructure information. This work was supported by grants from Alberta Health, and Public Health Agency of Canada.

## Author Contributions

J.L. prepared the original draft of the manuscript. J.L., K.X., E.A., S.S., N.A., J.V.D. and S.B. performed the primary investigation and method development aspects of the study. J.L., S.S., N.A., S.B., C.R.J.H. and M.D.P. contributed to visualization. J.L., N.A., K.F., C.R.J.H., B.E.L. X.P. and M.D.P. led the studies conceptualization. J.L., S.S., N.A. S.B., S.B., C.R.J.H and M.D.P. contributed to the initial data analyses. M.D.P, C.R.J.H., C.O., K.F. led the projects administration. M.D.P, C.R.J.H., K.F., B.E.L., X.P. acquired funding and supervised the project. All authors contributed to revising and creating the formal manuscript.

## Competing Interests

The authors declare no competing interests

## References

1. Collignon, P., Beggs, J. J., Walsh, T. R., Gandra, S. & Laxminarayan, R. Anthropological and socioeconomic factors contributing to global antimicrobial resistance: a univariate and multivariable analysis. *Lancet Planet. Health* **2**, e398-e405 (2018). [https://doi.org/10.1016/S2542-5196\(18\)30186-4](https://doi.org/10.1016/S2542-5196(18)30186-4)
2. Aslam, B., Khurshid, M., Arshad, M. I., Muzammil, S., Rasool, M., Yasmeen, N., Shah, T., Chaudhry, T. H., Rasool, M. H. & Shahid, A. Antibiotic resistance: one health one world outlook. *Front. Cell. Infect. Microbiol.*, 1153 (2021). <https://doi.org/10.3389/fcimb.2021.771510>
3. Murray, C. J., Ikuta, K. S., Sharara, F., Swetschinski, L., Aguilar, G. R., Gray, A., Han, C., Bisignano, C., Rao, P. & Wool, E. Global burden of bacterial antimicrobial resistance in 2019: a systematic analysis. *Lancet* **399**, 629-655 (2022). [https://doi.org/10.1016/S0140-6736\(21\)02724-0](https://doi.org/10.1016/S0140-6736(21)02724-0)
4. Maugeri, A., Barchitta, M., Puglisi, F. & Agodi, A. Socio-economic, governance and health indicators shaping antimicrobial resistance: an ecological analysis of 30 european countries. *Glob. Health* **19**, 12 (2023). <https://doi.org/10.1186/s12992-023-00913-0>
5. Hendriksen, R. S., Munk, P., Njage, P., Van Bunnik, B., McNally, L., Lukjancenko, O., Röder, T., Nieuwenhuijse, D., Pedersen, S. K. & Kjeldgaard, J. Global monitoring of antimicrobial resistance based on metagenomics analyses of urban sewage. *Nat. Commun.* **10**, 1124 (2019). <https://doi.org/10.1038/s41467-019-08853-3>
6. Prieto Riquelme, M. V., Garner, E., Gupta, S., Metch, J., Zhu, N., Blair, M. F., Arango-Argoty, G., Maile-Moskowitz, A., Li, A.-d. & Flach, C.-F. Demonstrating a Comprehensive Wastewater-Based Surveillance Approach That Differentiates Globally Sourced Resistomes. *Environ. Sci. Technol.* **56**, 14982-14993 (2022). <https://doi.org/10.1021/acs.est.1c08673>
7. Munk, P., Brinch, C., Møller, F. D., Petersen, T. N., Hendriksen, R. S., Seyfarth, A. M., Kjeldgaard, J. S., Svendsen, C. A., Van Bunnik, B. & Berglund, F. Genomic analysis of sewage from 101 countries reveals global landscape of antimicrobial resistance. *Nat. Commun.* **13**, 7251 (2022). <https://doi.org/10.1038/s41467-022-34312-7>
8. Wozniak, T. M., Cunningham, W., Ledingham, K. & McCulloch, K. Contribution of socio-economic factors in the spread of antimicrobial resistant infections in Australian primary healthcare clinics. *J. Global Antimicrob. Resist.* **30**, 294-301 (2022). <https://doi.org/10.1016/j.jgar.2022.06.005>



9. Honsbeek, M., Tjon-A-Tsien, A., Stobberingh, E., de Steenwinkel, J., Melles, D. C., Lous, J., Richardus, J. H. & Voeten, H. Low antimicrobial resistance in general practice patients in Rotterdam, the city with the largest proportion of immigrants in the Netherlands. *Eur. J. Clin. Microbiol. Infect. Dis.* **39**, 929-935 (2020). <https://doi.org/10.1007/s10096-019-03804-8>
10. King, T., Schindler, R., Chavda, S. & Conly, J. Dimensions of poverty as risk factors for antimicrobial resistant organisms in Canada: a structured narrative review. *Antimicrob. Resist. Infect. Control* **11**, 18 (2022). <https://doi.org/10.1186/s13756-022-01059-1>
11. Aarestrup, F. M. & Woolhouse, M. E. Using sewage for surveillance of antimicrobial resistance. *Science* **367**, 630-632 (2020). <https://doi.org/10.1126/science.aba3432>
12. Adebisi, Y. A. & Ogunkola, I. O. The global antimicrobial resistance response effort must not exclude marginalised populations. *Trop. Med. Health* **51**, 33 (2023). <https://doi.org/10.1186/s41182-023-00524-w>
13. Sims, N. & Kasprzyk-Hordern, B. Future perspectives of wastewater-based epidemiology: monitoring infectious disease spread and resistance to the community level. *Environ. Int.* **139**, 105689 (2020). <https://doi.org/10.1016/j.envint.2020.105689>
14. Calgary. 2019 Civic Census Results. <https://www.calgary.ca/content/dam/www/ca/city-clerks/documents/election-and-information-services/census2019/2019-censusresultsbook.pdf>. Retrieved 2022 October 26. (2019).
15. Statistics-Canada. Table 23-10-0253-01 Air passenger traffic at Canadian airports, annual, Statistics Canada. Retrieved at September 13, 2023. <https://doi.org/10.25318/2310025301-eng>. (2023).
16. Spigaglia, P., Carucci, V., Barbanti, F. & Mastrantonio, P. ErmB determinants and Tn 916-like elements in clinical isolates of *Clostridium difficile*. *Antimicrob. Agents Chemother.* **49**, 2550-2553 (2005). <https://doi.org/10.1128/aac.49.6.2550-2553.2005>
17. Wu, J.-J., Ko, W.-C., Tsai, S.-H. & Yan, J.-J. Prevalence of plasmid-mediated quinolone resistance determinants QnrA, QnrB, and QnrS among clinical isolates of *Enterobacter cloacae* in a Taiwanese hospital. *Antimicrob. Agents Chemother.* **51**, 1223-1227 (2007). <https://doi.org/10.1128/aac.01195-06>
18. Monte, D. F., Sellera, F. P., Lopes, R., Keelara, S., Landgraf, M., Greene, S., Fedorka-Cray, P. J. & Thakur, S. Class 1 integron-borne cassettes harboring bla CARB-2 gene in multidrug-resistant and virulent *Salmonella* Typhimurium ST19 strains recovered from clinical human stool samples, United States. *PLoS One* **15**, e0240978 (2020). <https://doi.org/10.1371/journal.pone.0240978>
19. Abrar, S., Ain, N. U., Liaqat, H., Hussain, S., Rasheed, F. & Riaz, S. Distribution of bla CTX-M, bla TEM, bla SHV and bla OXA genes in Extended-spectrum- $\beta$ -lactamase-producing Clinical isolates: A three-year multi-center study from Lahore, Pakistan. *Antimicrob. Resist. Infect. Control* **8**, 1-10 (2019). <https://doi.org/10.1186/s13756-019-0536-0>
20. UNDP. Human Development Reports, United Nations Development Programme (UNDP). Retrieved at September 13, 2023. <https://hdr.undp.org/>. (2023).
21. Allel, K., Labarca, J., Carvajal, C., Garcia, P., Cifuentes, M., Silva, F., Munita, J. M. & Undurraga, E. A. Trends and socioeconomic, demographic, and environmental factors associated with antimicrobial resistance: a longitudinal analysis in 39 hospitals in Chile 2008–2017. *Lancet Reg. Health -Americas* **21** (2023). <https://doi.org/10.1016/j.lana.2023.100484>

22. Neves, F. P. G., Marlow, M. A., Rezende-Pereira, G., Pinheiro, M. G., Dos Santos, A. F. M., de Fátima Nogueira de Freitas, M., Barros, R. R., Aguiar-Alves, F., Cardoso, C. A. A. & Riley, L. W. Differences in gram-positive bacterial colonization and antimicrobial resistance among children in a high income inequality setting. *BMC Infect. Dis.* **19**, 1-9 (2019). [https://doi.org:https://doi.org/10.1186/s12879-019-4104-2](https://doi.org/https://doi.org/10.1186/s12879-019-4104-2)
23. Rios, G., Lacoux, C., Leclercq, V., Diamant, A., Lebrigand, K., Lazuka, A., Soyeux, E., Lacroix, S., Fassy, J. & Couesnon, A. Monitoring SARS-CoV-2 variants alterations in Nice neighborhoods by wastewater nanopore sequencing. *Lancet Reg. Health -Europe* **10** (2021). <https://doi.org:https://doi.org/10.1016/j.lanepe.2021.100202>
24. Acosta, N., Bautista, M. A., Waddell, B. J., McC Calder, J., Beaudet, A. B., Man, L., Pradhan, P., Sedaghat, N., Papparis, C. & Bacanu, A. Longitudinal SARS-CoV-2 RNA Wastewater Monitoring Across a Range of Scales Correlates with Total and Regional COVID-19 Burden in a Well-Defined Urban Population. *Water Res.*, 118611 (2022). <https://doi.org:https://doi.org/10.1016/j.watres.2022.118611>
25. Prasek, S. M., Pepper, I. L., Innes, G. K., Slinski, S., Ruedas, M., Sanchez, A., Brierley, P., Betancourt, W. Q., Stark, E. R. & Foster, A. R. Population level SARS-CoV-2 fecal shedding rates determined via wastewater-based epidemiology. *Sci. Total Environ.* **838**, 156535 (2022). <https://doi.org:https://doi.org/10.1016/j.scitotenv.2022.156535>
26. Van Ham, M., Tammaru, T., Ubarevičienė, R. & Janssen, H. *Rising inequalities and a changing social geography of cities. An introduction to the global segregation book.* (Springer, 2021).
27. Statistics-Canada. Income inequality highest in Toronto, Calgary and Vancouver, Statistics-Canada. Retrieved at July 31 2023. <https://www150.statcan.gc.ca/n1/daily-quotidien/220713/g-d007-eng.htm>. (2023).
28. Government-of-Canada. Government extends international travel restrictions, Government of Canada, Retrieved at Jan 29 2024. <https://www.canada.ca/en/public-safety-canada/news/2020/10/government-extends-international-travel-restrictions.html>. (2020).
29. Bokhary, H., Pangesti, K. N., Rashid, H., Abd El Ghany, M. & Hill-Cawthorne, G. A. Travel-related antimicrobial resistance: a systematic review. *Trop. Med. Infect. Dis.* **6**, 11 (2021). <https://doi.org:https://doi.org/10.3390/tropicalmed6010011>
30. Heaton, K., Radvan, J., Cripps, H., Mountford, R., Braddon, F. & Hughes, A. Defecation frequency and timing, and stool form in the general population: a prospective study. *Gut* **33**, 818 (1992). <https://doi.org:https://doi.org/10.1136/gut.33.6.818>
31. CDC. Core Elements of Hospital Antibiotic Stewardship Programs. The US Center for Disease Control and Prevention (CDC), Retrieved at Nov 22 2023. <https://www.cdc.gov/antibiotic-use/core-elements/hospital.html>. (2023).
32. Leis, J. A., Born, K. B., Ostrow, O., Moser, A. & Grill, A. Prescriber-led practice changes that can bolster antimicrobial stewardship in community health care settings. *Commun. Dis. Rep.* **46**, 1-5 (2020). <https://doi.org:https://doi.org/10.14745/ccdr.v46i01a01>
33. Klein, E. Y., Van Boeckel, T. P., Martinez, E. M., Pant, S., Gandra, S., Levin, S. A., Goossens, H. & Laxminarayan, R. Global increase and geographic convergence in antibiotic consumption between 2000 and 2015. *PNAS* **115**, E3463-E3470 (2018). <https://doi.org:https://doi.org/10.1073/pnas.1717295115>
34. AHS. Alberta Health Services (AHS), AHS. Retrieved at Nov 23, 2023. <https://www.albertahealthservices.ca>. (2023).

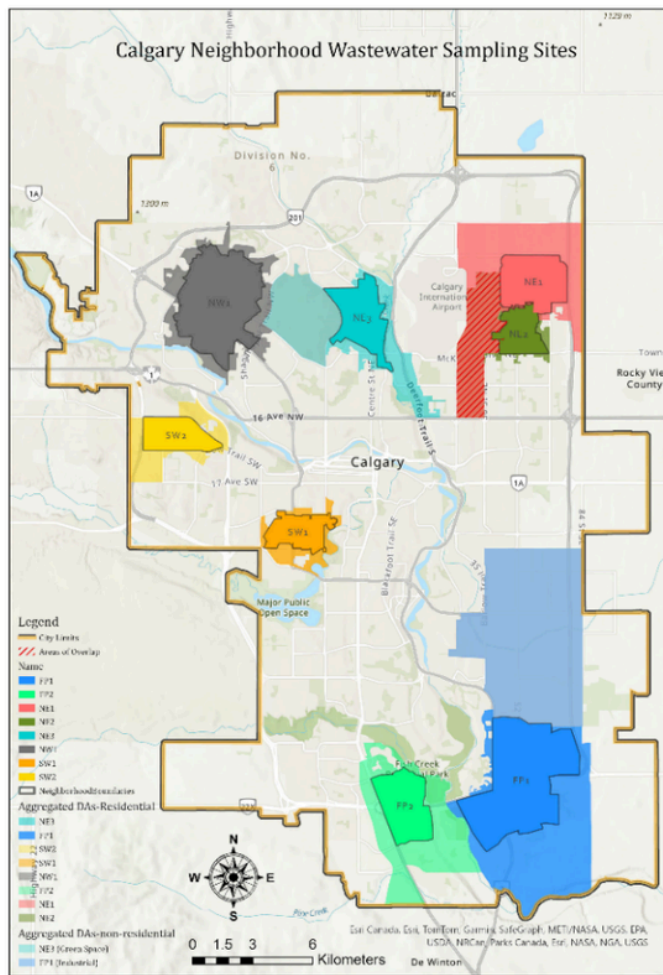
35. Peters, D. H., Garg, A., Bloom, G., Walker, D. G., Brieger, W. R. & Hafizur Rahman, M. Poverty and access to health care in developing countries. *Ann. N. Y. Acad. Sci.* **1136**, 161-171 (2008).  
<https://doi.org/https://doi.org/10.1196/annals.1425.011>
36. World-Bank. World Bank Open Data, WorldBank. Retrieved at September 13, 2023.  
<https://data.worldbank.org/>. (2023).
37. Peirano, G., Gregson, D. B., Kuhn, S., Vanderkooi, O. G., Nobrega, D. B. & Pitout, J. D. Rates of colonization with extended-spectrum  $\beta$ -lactamase-producing *Escherichia coli* in Canadian travellers returning from South Asia: a cross-sectional assessment. *CMAJ open* **5**, E850-E855 (2017).  
<https://doi.org/https://doi.org/10.9778/cmajo.20170041>
38. Peirano, G., Ahmed-Bentley, J., Fuller, J., Rubin, J. E. & Pitout, J. D. Travel-related carbapenemase-producing Gram-negative bacteria in Alberta, Canada: the first 3 years. *J. Clin. Microbiol.* **52**, 1575-1581 (2014).  
<https://doi.org/https://doi.org/10.1128/jcm.00162-14>
39. Hung, K., Xiao, H. & Yang, X. Why immigrants travel to their home places: Social capital and acculturation perspective. *Tour. Manag.* **36**, 304-313 (2013).  
<https://doi.org/https://doi.org/10.1016/j.tourman.2012.12.010>
40. Government-of-Canada. Antimicrobial use (AMU) in the Canadian community sector, Government of Canada, Retrieved at Jan 29 2024. <https://health-infobase.canada.ca/carss/> (2023).
41. Knight, B. D., Shurgold, J., Smith, G., MacFadden, D. R., Schwartz, K. L., Daneman, N., Tropper, D. G. & Brooks, J. The impact of COVID-19 on community antibiotic use in Canada: an ecological study. *Clin. Microbiol. Infect.* **28**, 426-432 (2022). <https://doi.org/https://doi.org/10.1016/j.cmi.2021.10.013>
42. Nandi, A., Pecetta, S. & Bloom, D. E. Global antibiotic use during the COVID-19 pandemic: Analysis of pharmaceutical sales data from 71 countries, 2020–2022. *eClinicalMedicine* **57** (2023).  
<https://doi.org/https://doi.org/10.1016/j.eclinm.2023.101848>
43. Mancuso, G., Midiri, A., Gerace, E. & Biondo, C. Bacterial antibiotic resistance: The most critical pathogens. *Pathogens* **10**, 1310 (2021). <https://doi.org/https://doi.org/10.3390/pathogens10101310>
44. PHAC. Canadian Antimicrobial Resistance Surveillance System Report 2022, Public Health Agency of Canada (PHAC), Retrieved at Aug 01 2023 <https://www.canada.ca/en/public-health/services/publications/drugs-health-products/canadian-antimicrobial-resistance-surveillance-system-report-2022.html>. (2022).
45. Browne, A. J., Chipeta, M. G., Haines-Woodhouse, G., Kumaran, E. P., Hamadani, B. H. K., Zaraa, S., Henry, N. J., Deshpande, A., Reiner, R. C. & Day, N. P. Global antibiotic consumption and usage in humans, 2000–18: a spatial modelling study. *Lancet Planet. Health* **5**, e893-e904 (2021).  
[https://doi.org/https://doi.org/10.1016/S2542-5196\(21\)00280-1](https://doi.org/https://doi.org/10.1016/S2542-5196(21)00280-1)
46. Crosby, M., von den Baumen, T. R., Chu, C., Gomes, T., Schwartz, K. L. & Tadrous, M. Interprovincial variation in antibiotic use in Canada, 2019: a retrospective cross-sectional study. *CMAJ open* **10**, E262-E268 (2022).  
<https://doi.org/https://doi.org/10.9778/cmajo.20210095>
47. UofC. Urban Alliance - A strategic partnership between The City of Calgary and University of Calgary, University of Calgary (UofC). Retrieved at Sept 19, 2021. <https://research.ucalgary.ca/urban-alliance/home>. (2021).

48. Statistics-Canada. Census Profile, 2021 Census of Population, Statistics-Canada, Retrieved at Nov 22 2023. <https://www12.statcan.gc.ca/census-recensement/2021/dp-pd/prof/details/download-telecharger.cfm?Lang=E>. (2023).
49. Crossman, E. Low-income and immigration: An overview and future directions for research. Citizenship and Immigration Canada. Retrieved at Sept 10 2023. <https://www.canada.ca/content/dam/ircc/migration/ircc/english/resources/research/documents/pdf/r21-2012-low-income-ec-eng.pdf>. (2013).
50. Rodriguez-R, L. M., Gunturu, S., Tiedje, J. M., Cole, J. R. & Konstantinidis, K. T. Nonpareil 3: fast estimation of metagenomic coverage and sequence diversity. *MSystems* **3**, e00039-00018 (2018). <https://doi.org/https://doi.org/10.1128/msystems.00039-18>
51. Andrews, S. FastQC: A Quality Control Tool for High Throughput Sequence Data [Online]. Available online at: <http://www.bioinformatics.babraham.ac.uk/projects/fastqc/>. (2010).
52. Bolger, A. M., Lohse, M. & Usadel, B. Trimmomatic: a flexible trimmer for Illumina sequence data. *Bioinformatics* **30**, 2114-2120 (2014). <https://doi.org/https://doi.org/10.1093/bioinformatics/btu170>
53. Arango-Argoty, G., Garner, E., Pruden, A., Heath, L. S., Vikesland, P. & Zhang, L. DeepARG: a deep learning approach for predicting antibiotic resistance genes from metagenomic data. *Microbiome* **6**, 23 (2018). <https://doi.org/https://doi.org/10.1186/s40168-018-0401-z>
54. Acosta, N., Lee, J., Bautista, M., Bhatnagar, S., Waddell, B., Au, E., Pradhan, P., Clark, R., Achari, G. & Pitout, J. D. Metagenomic analysis after selective culture enrichment of wastewater demonstrates increased burden of antibiotic resistant genes in hospitals relative to the community. *medRxiv*, 2023.2003.2007.23286790 (2023). <https://doi.org/https://doi.org/10.1101/2023.03.07.23286790>
55. Keenum, I., Williams, R. K., Ray, P., Garner, E. D., Knowlton, K. F. & Pruden, A. Combined effects of composting and antibiotic administration on cattle manure-borne antibiotic resistance genes. *Microbiome* **9**, 1-16 (2021). <https://doi.org/https://doi.org/10.1186/s40168-021-01006-z>
56. Lee, J., Ju, F., Maile-Moskowitz, A., Beck, K., Maccagnan, A., McArdell, C. S., Dal Molin, M., Fenicia, F., Vikesland, P. J., Pruden, A., Stamm, C. & Burgmann, H. Unraveling the riverine antibiotic resistome: The downstream fate of anthropogenic inputs. *Water Res.* **197**, 117050 (2021). <https://doi.org/https://doi.org/10.1016/j.watres.2021.117050>
57. Colomer-Lluch, M., Jofre, J. & Muniesa, M. Quinolone resistance genes (qnrA and qnrS) in bacteriophage particles from wastewater samples and the effect of inducing agents on packaged antibiotic resistance genes. *J. Antimicrob. Chemother.* **69**, 1265-1274 (2014). <https://doi.org/https://doi.org/10.1093/jac/dkt528>
58. Lachmayr, K. L., Kerkhof, L. J., DiRienzo, A. G., Cavanaugh, C. M. & Ford, T. E. Quantifying nonspecific TEM  $\beta$ -lactamase (bla TEM) genes in a wastewater stream. *Appl. Environ. Microbiol.* **75**, 203-211 (2009). <https://doi.org/https://doi.org/10.1128/AEM.01254-08>
59. Nadkarni, M. A., Martin, F. E., Jacques, N. A. & Hunter, N. Determination of bacterial load by real-time PCR using a broad-range (universal) probe and primers set. *Microbiology* **148**, 257-266 (2002). <https://doi.org/https://doi.org/10.1099/00221287-148-1-257>
60. Bustin, S. A., Benes, V., Garson, J. A., Hellemans, J., Huggett, J., Kubista, M., Mueller, R., Nolan, T., Pfaffl, M. W. & Shipley, G. L. The MIQE Guidelines: Minimum Information for Publication of Quantitative Real-Time PCR Experiments. *Clin. Chem.* **55**, 611-622 (2009). <https://doi.org/https://doi.org/10.1373/clinchem.2008.112797>

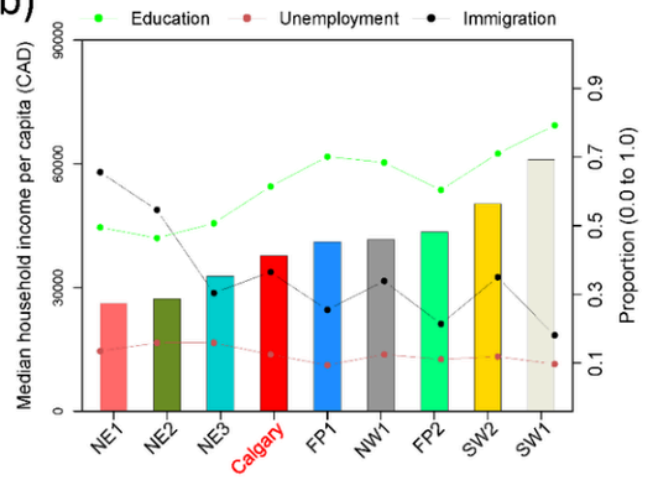
61. Nolan, T., Hands, R. E. & Bustin, S. A. Quantification of mRNA using real-time RT-PCR. *Nat. Protoc.* **1**, 1559-1582 (2006). <https://doi.org/10.1038/nprot.2006.236>
62. Li, H. seqtk Toolkit for processing sequences in FASTA/Q formats. (2012). <https://github.com/lh3/seqtk>
63. Stein-Thoeringer, C. K., Saini, N. Y., Zamir, E., Blumenberg, V., Schubert, M.-L., Mor, U., Fante, M. A., Schmidt, S., Hayase, E. & Hayase, T. A non-antibiotic-disrupted gut microbiome is associated with clinical responses to CD19-CAR-T cell cancer immunotherapy. *Nat. Med.*, 1-11 (2023). <https://doi.org/10.1038/s41591-023-02234-6>
64. Maciel-Guerra, A., Baker, M., Hu, Y., Wang, W., Zhang, X., Rong, J., Zhang, Y., Zhang, J., Kaler, J. & Renney, D. Dissecting microbial communities and resistomes for interconnected humans, soil, and livestock. *ISME J.* **17**, 21-35 (2023). <https://doi.org/10.1038/s41396-022-01315-7>
65. R-Core-Team. Package 'stats'. (2022). <https://stat.ethz.ch/R-manual/R-devel/library/stats/html/00Index.html>
66. Oksanen, J., Blanchet, F. G., Kindt, R., Legendre, P., Minchin, P. R., O'hara, R., Simpson, G. L., Solymos, P., Stevens, M. H. H. & Wagner, H. Package 'vegan'. (2022). <https://cran.r-project.org/web/packages/vegan/vegan.pdf>
67. Garcia, L. & Lorena, A. Package 'ECoL'. (2022). <https://cran.r-project.org/web/packages/ECoL/ECoL.pdf>
68. Ter Braak, C. J. & Prentice, I. C. in *Adv. Ecol. Res.* Vol. 18 271-317 (Elsevier, 1988).
69. Warnes, M. G. R., Bolker, B., Bonebakker, L., Gentleman, R. & Huber, W. Package 'gplots'. (2022). <https://cran.r-project.org/web/packages/gplots/gplots.pdf>
70. Lee, J., Acosta, N., Waddell, B. J., Du, K., Xiang, K., Van Doorn, J., Low, K., Bautista, M. A., McCaLder, J., Dai, X., Lu, X., Chekouo, T., Pradhan, P., Sedaghat, N., Papparis, C., Beaudet, A. B., Chen, J., Chan, L., Vivas, L., Westlund, P., Bhatnagar, S., Stefani, S., Visser, G., Cabaj, J., Bertazzon, S., Sarabi, S., Achari, G., Clark, R., Hruday, S. E., Lee, B. E., Pang, X., Webster, B., Ghali, W. A., Buret, A. G., Williamson, T., Southern, D. A., Meddings, J., Frankowski, K., Hubert, C. & Parkins, M. Campus node-based wastewater surveillance enables COVID-19 case localization and confirms lower SARS-CoV-2 burden relative to the surrounding community. *Water Res.* **244**, 120469 (2023). <https://doi.org/10.1016/j.watres.2023.120469>

## Figures

(a)



(b)



(c)



Figure 1

**Sampling map and socio-economic status (SES) indicators of Calgary neighbourhoods.** (a) Map showing the city of Calgary and eight neighborhood sampling sites (differently coloured), intersected with Dissemination Areas (DAs), i.e., spatial units where SES variables are surveyed (Census data). In cases of DAs only partially overlapping sewersheds, sewersheds are shown in opaque, darker colours, whereas the residual portions of DAs are shown in lighter, more transparent colors (see Methods 4.2 for details); the cross-hatched areas indicate the residual portions of DAs that partially overlap with two sewersheds, i.e., NE1 and NE2; (b) Histogram of SES data on income, education, unemployment and immigration variables derived from Statistics Canada’s 2021 Census for those eight neighbourhoods (colours corresponding to the map) as well as Calgary as a whole (bright red; median); (c) Correlations (Spearman’s) across SES variables, with positive correlations represented by blue shades, and negative ones by red shades. p-values corrected by the Benjamini-Hochberg procedure for multiple comparisons are reported in each cell.

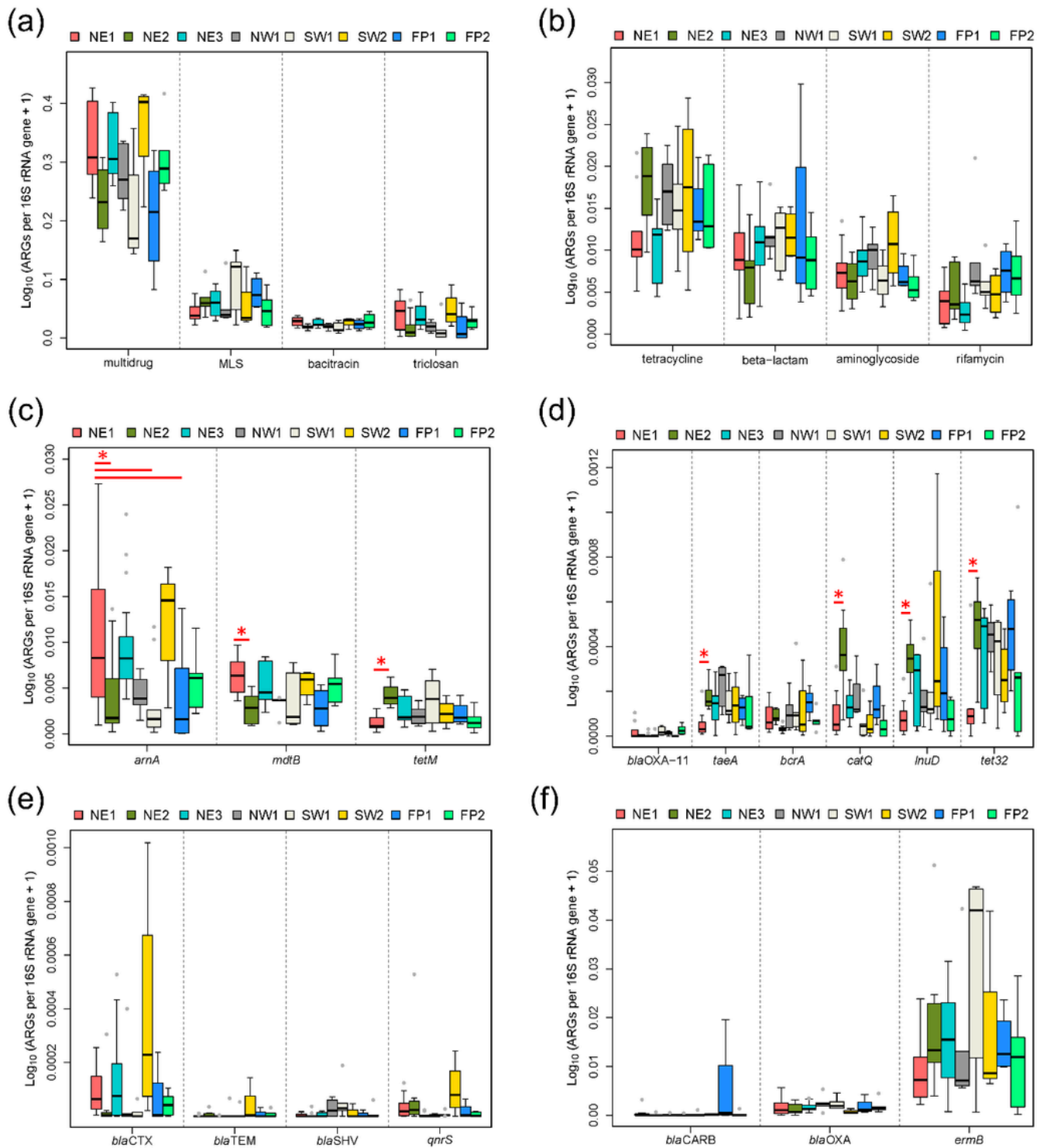


**Figure 2**

**Log-transformed relative abundance of antibiotic resistance genes (ARGs) across eight different neighbourhoods.** (a-b) Eight most abundant ARG-types found in neighbourhood samples; (c-d) Nine ARG-subtypes that differed significantly between neighbourhoods based on Wilcoxon rank-sum tests, where (c) are more prevalent ARGs, and (d) are less prevalent ARGs based upon relative abundance; (e-f) selected ARG-subtypes of specific clinical importance displayed in panels, where (e) are more prevalent ARGs, and (f) are less

prevalent ARGs based upon relative abundance. The neighbourhoods that significantly differed from NE1 for a given ARG were denoted by asterisks (\*), with results for other test-pairs shown in Tables S1.

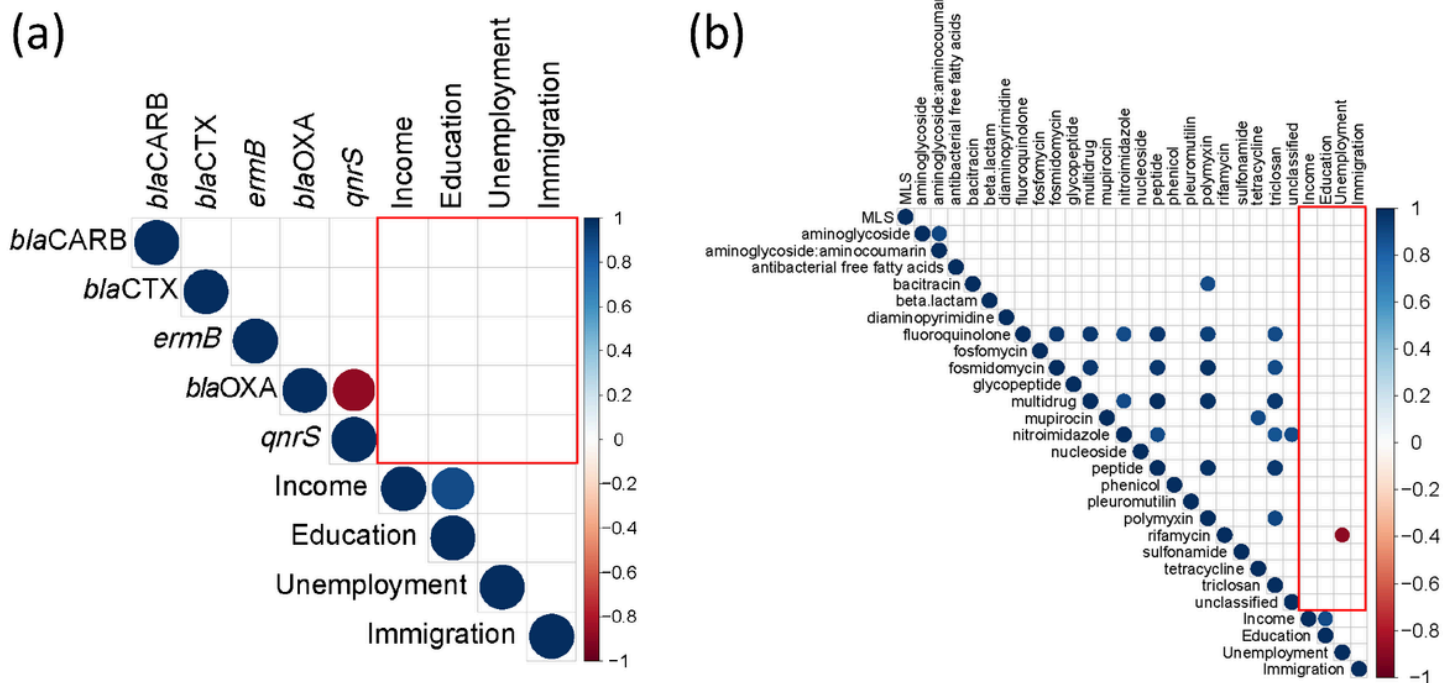
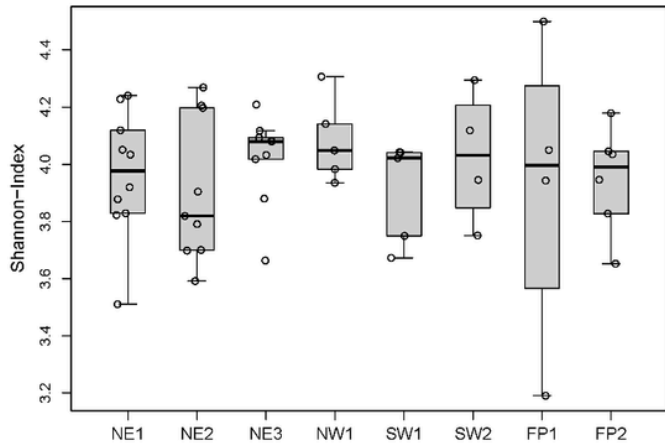


**Figure 3**

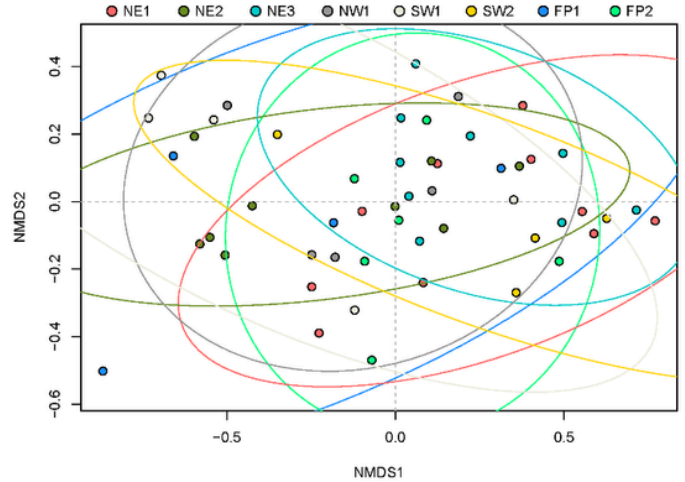
**Relationships between socioeconomic status (SES) and the resistome.** Pairwise correlation between four SES variables and (a) five specific ARGs having clinical importance, and (b) a longer list including major ARG types identified in this study, with  $r$  values colored in a diverging color scale (blue for positive, red for negative correlation), also  $p_{\text{adj}} < 0.10$  were shown. The pairs between SES and ARGs were located within the red-coloured box (where  $p_{\text{adj}}$  for rifamycin-unemployment 0.06). MLS denotes macrolide-lincosamide-streptogramin.



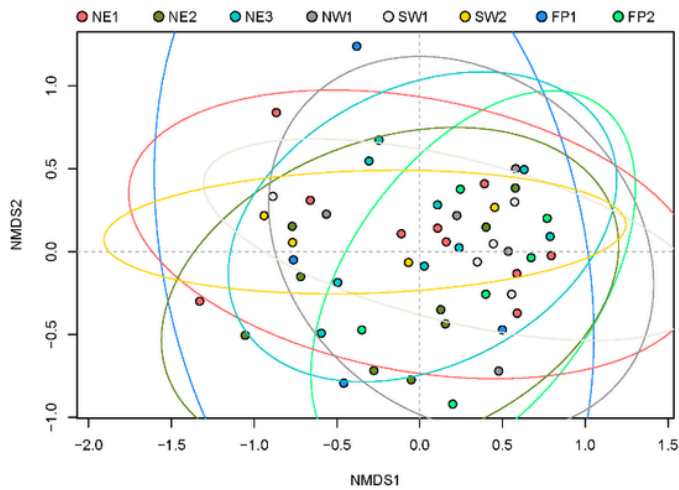
(a) alpha-diversity



(b) total ARGs



(c) beta-lactam antibiotics



(d) beta-lactamases

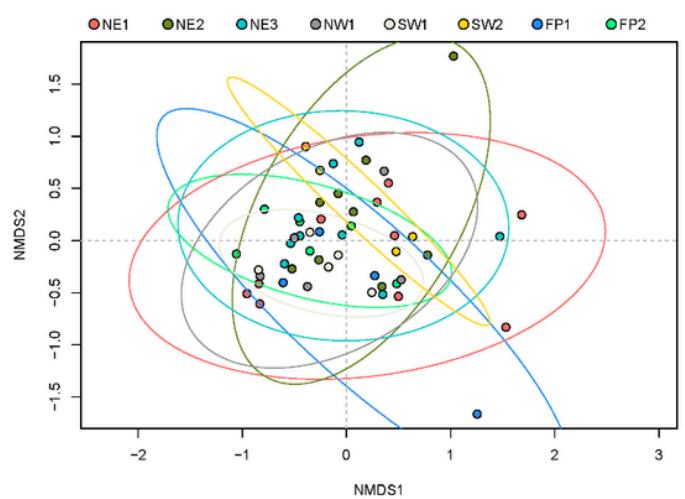


**Figure 4**

**Resistomes of eight Calgary neighbourhoods.** Resistome alpha-diversity represented by Shannon Index values (a) and beta-diversity visualized by non-metric multidimensional scaling (NMDS) (b-d) based on analysis of ARGs from eight different neighbourhoods. Beta diversity was compared based on calculations for the entire resistome (b) and only for beta-lactam antibiotic resistance genes (c) and beta-lactamase genes (d). Variance ellipses indicated standard deviations of ordination scores (confidence limit=0.95).

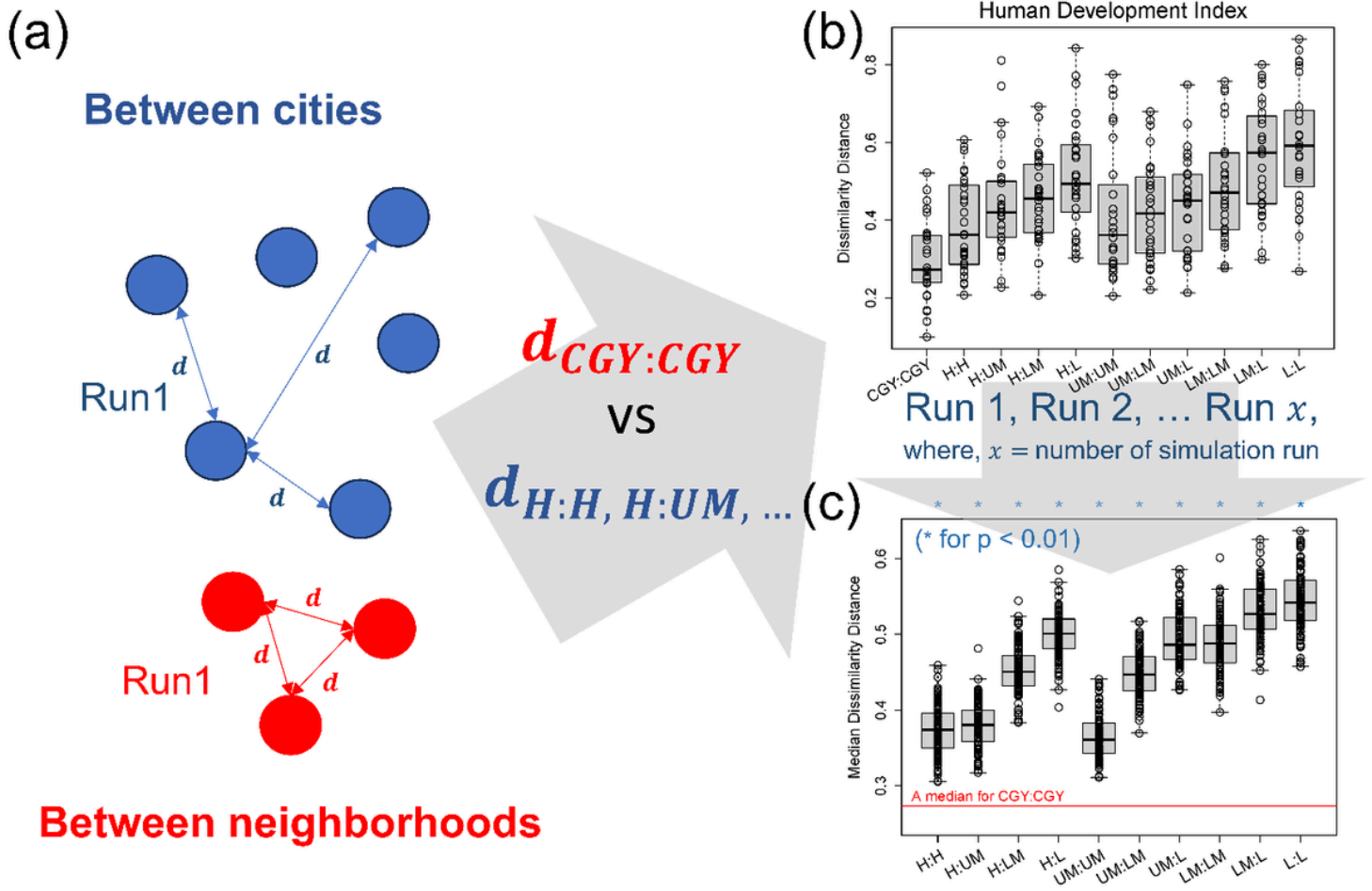
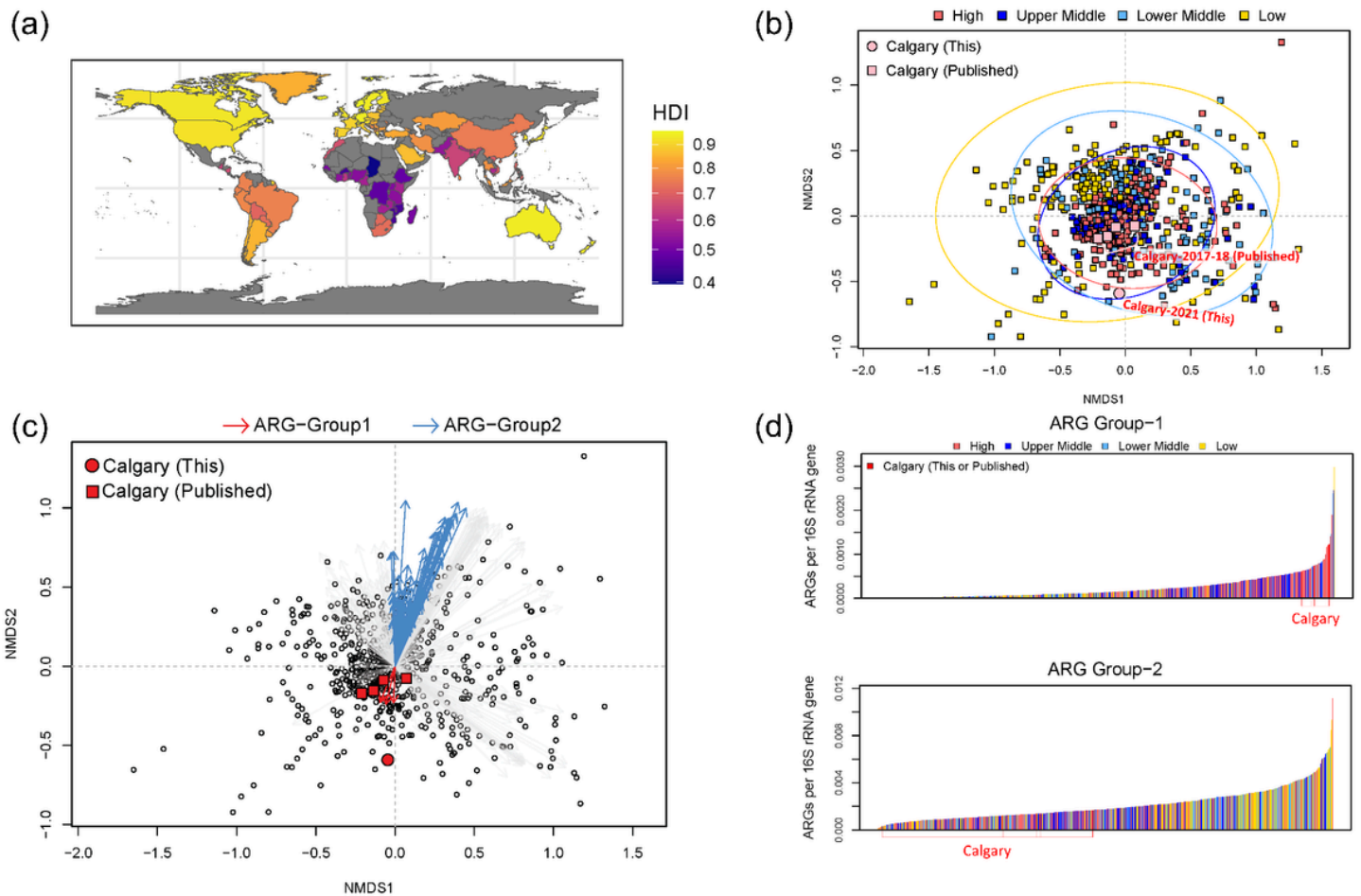


Figure 5

Schematic depicting workflow for comparing dissimilarity between resistomes in wastewater from Calgary and other locations around the world, categorized by Human Development Index (HDI). (a) A diagram describing a random selection of certain number ( $n=28$ ) of dissimilarity distance,  $d$  in a single run, (b-c) comparisons of dissimilarity distance between Calgary neighbourhoods (CGY:CGY) and between cities with different HDI classifications (b) in a single run and (c) and in multiple runs. Calculated p-values according to (Eq. 6) are denoted by asterisks (\*) in (c). Classifications of global cities used in this analysis include high (H), upper-middle (UM), lower-middle (LM), and low (L)-categories based on HDI (see Fig. S12 and Methods 4.7 for details).



**Figure 6**

**Analysis of globally-sourced metagenomes.** (a) Map showing the Human Development Index (HDI) of the cities examined in this study. The HDI value of each global city is ascribed from its resident country; (b) Beta-diversity analysis visualised by NMDS with colours and ellipses (standard deviation of ordination scores; 0.95 confidence limit) denoting high, upper-middle, bottom-middle and low categories for HDI; (c) Biplot analysis of the top 100 ARGs most correlated with Calgary wastewater samples (from this, also published studies) shown in thick red (for positively associated genes; Group-1) or blue (for negatively associated genes; Group-2), and otherwise in light grey arrows; (d) Combined relative abundances of ARGs normalized against 16S rRNA genes across samples for Group-1 and Group-2.

## Supplementary Files

This is a list of supplementary files associated with this preprint. Click to download.

- [Mar31.SupplementaryInformationforWBSMetagenomeNeighborhoodv11Cleaned.docx](#)